Propagation of light pulses in a $(j_1=\frac{1}{2})-(j_2=\frac{1}{2})$ medium in the sharp-line limit

Abu Mohamed Alhasan*

Institute of Physics, Faculty of Mathematics and Natural Sciences, Pomeranian University in Słupsk, Arciszewskiego 22b, 76-200 Słupsk, Poland

Janusz Czub† and Wiesław Miklaszewski‡

Instytut Fizyki Teoretycznej i Astrofizyki, Uniwersytet Gdański, ul. Wita Stwosza 57, 80-952 Gdańsk, Poland

(Received 22 June 2009; published 4 September 2009)

The analytical and numerical study of the propagation of elliptically polarized light in the medium composed of fixed $(j_1=\frac{1}{2})-(j_2=\frac{1}{2})$ atoms is presented. Properties of the ringing produced by light pulses are analyzed. The stabilization of the total propagating field area is presented. The redistribution of the energy between two phase shifted laser fields with orthogonal linear polarizations is investigated.

DOI: 10.1103/PhysRevA.80.033809 PACS number(s): 42.50.Gy, 42.50.Hz, 42.65.Re

I. INTRODUCTION

The short light pulse propagation in the medium composed of two-level atoms has been a subject of intensive research for many years. This phenomenon is usually described theoretically by the Maxwell-Bloch equations [1]. When the medium is inhomogeneously broadened and the atomic damping is negligible, the well-known self-induced transparency effect (SIT) can be observed [2]. The explanation of the SIT effect is based on the area theorem which is obtained in the framework of the rotating wave approximation (RWA) and the slowly varying envelope approximation.

If the inhomogeneous broadening, the atomic relaxation, and the pulse phase are neglected, the resonant pulse propagation is governed by the sine-Gordon equation [1,3,4]. Such a model, called a sharp-line case [3], a fixed atoms case [4] or a soluble model [1] seemed to be far from experimental reality. However, numerical calculations showed that effects predicted on the basis of this model are still present when the inhomogeneous broadening is involved [1,4]. Moreover a sharp-line SIT, in which ratio of pulse width to linewidth is much greater than one, was observed [5,6]. Quite recently the development of laser cooling and trapping techniques enabled preparation of a medium with negligible inhomogeneous width and density high enough for pulse propagation experiments [7,8].

When the propagation of nanosecond or longer pulses is considered, the atomic relaxation due to spontaneous emission and collision processes have to be taken into account and the relaxation rates should be included in Bloch equations [9]. In such a case the Maxwell-Bloch equations can be solved analytically only in the weak-field limit or for small area pulses [10,11]. The propagating light pulse induces a dipole moment in the medium which decays due to perpendicular relaxation and inhomogeneous dephasing. This effect is called optical free-induction decay (FID) [12]. The induced dipole moment causes the Burnham-Chio ringing [13] (in the limit of infinite relaxation time and negligible pulse attenuation) or optical ringing [14].

Since the optical ringing decays in time much longer than the ultrashort pulse duration, the propagation of such a pulse and formation of the free-induction field are usually treated independently. The combined approach was presented in [15,16]. It was shown numerically that in the sharp-line limit total resonant light field, the pulse and the ringing form the optical transient with the area equal to $2n\pi$ during propagation in the two-level medium. This area is stable until the losses due to the spontaneous emission cause its jump to the lower value $2(n-1)\pi$. This process repeats until a 0π pulse is formed. When the input pulses are short enough the optical ringing is responsible for the field area stabilization at least for small propagation distances. In other words the joined area of the free-induction field and of the pulse is equal to $2n\pi$.

In the standard treatment of the SIT problem the spatial level degeneracy is rarely considered. When the light is polarized it should be taken into account. However, if the linearly polarized light is applied the system $j_1=1/2-j_2=1/2$ behaves like a two-level atom [15,16]. Obviously the linearly polarized light can be understood as a superposition of two components with orthogonal circular polarizations and equal intensities. In general, these two components with unequal intensities form elliptically polarized light. Recently the propagation of two femtosecond pulses with perpendicular linear polarizations in the $j_1=1/2-j_2=1/2$ medium was studied experimentally and theoretically [17–20]. One of these pulses was strong and the other weak. It was demonstrated that the medium gain for the weak one can be efficiently controlled. The obtained results were explained by interference between the different absorption and stimulated emission paths for weak pulse photons.

In this paper we study the propagation of elliptically polarized field in the $j_1=1/2-j_2=1/2$ medium, for example in the alkali-metal atom vapor, using the approach presented in [15,16]. More precisely, we consider the propagation of two fields with orthogonal circular polarizations. They are coupled only by the atomic relaxation, i.e., the spontaneous decay and collisional damping of the orientation in the upper state. Since the cross section for the spin flip in the ground

*alhasan@apsl.edu.pl

†fizjc@univ.gda.pl

‡fizwm@univ.gda.pl

state of the alkali-metal atom is very small [21], we neglect the orientation damping in the lower level. The dynamics of the atomic system is described by the density matrix in the irreducible spherical tensor representation [22].

The systems $j_1=1/2-j_2=1/2$, $j_1=0-j_2=1$, and $j_1=1-j_2=0$ are the simplest atomic systems with spatial level degeneracy. The understanding of their interaction with light is necessary for the construction of devices, allowing the coherent storage of information [23,24]. The effects accompanying the propagation of light in the atomic medium are important for quantum memory operation because the storage of light is achieved by controlling the spatial distribution of atomic states.

The paper is organized as follows. In Sec. II we present theoretical description of the excitation of the $j_1=1/2-j_2=1/2$ system by two near-resonant light fields with left and right circular polarizations We neglect the hyperfine structure and the motion of the atom, i.e., we neglect the redistribution of the atomic transition frequencies due to the Doppler effect. In Sec. III we study the properties of the area of free-induction field. In Sec. IV we present numerical results concerning the propagation of circularly polarized pulses. The redistribution of the energy between linearly polarized components of elliptically polarized light is investigated in Sec. V. We summarize the discussion in Sec VI.

II. THEORETICAL MODEL

In the description of the interaction of polarized light with a real atom, the spatial degeneracy of the atomic levels and atomic relaxation processes have to be taken into account. The most fruitful approach which includes them and allows describing the evolution of a system composed of an atom and electromagnetic field involves the density matrix and the Liouville space formalisms [22,25–27].

When an atom is immersed in a spherically symmetric thermal bath, representing the collisions with the buffer gas atoms, it is convenient to use as a basis of the Liouville space the rotationally irreducible set of atomic states [25,27]. From this set in some cases one can generate a reduced (minimal) basis sufficient for the complete description of the atom interacting with the polarized light [22]. The elements of such a basis are contractions of spherical tensors, constructed from the polarization vectors, and elements of the rotationally irreducible atomic basis.

The reduced density matrix ρ is expanded in the minimal basis $\{e_i\}$ according to

$$\rho = \sum_i \rho_i e_i, \tag{1}$$

and its time evolution is described by the Liouville equation [22],

$$i\frac{d}{dt}\rho = \hat{L}\rho = [H,\rho] + i\hat{\Phi}\rho = (-\hat{H} + i\hat{\Phi})\rho, \tag{2}$$

where $\hat{L}$ and $H=H_A+V$ denote the Liouvillian and the Hamiltonian of the system, respectively (we put $\hbar=1$). The operator H_A stands for the atomic Hamiltonian and V represents the interaction of the atom with the light beam

$$V = -\boldsymbol{\mu_D}\cdot\boldsymbol{E}, \tag{3}$$

where $\boldsymbol{E}$ denotes the electric field, whereas $\boldsymbol{\mu_D}$ is the atomic electric-dipole operator. In our approach the relaxation operator $\hat{\Phi}$ is determined phenomenologically by spontaneous damping rates and experimental collisional cross sections.

The dimension of the basis $\{e_i\}$ and the form of its elements depend on the level structure of the considered atom, on its initial state, and on the polarization vectors of light driving the atom. As a rule it is assumed that initially the atom is in the ground state with equally populated Zeeman sublevels. Since the dimension of the reduced basis for multilevel systems is usually large, it is practically impossible to solve Eq. (2) analytically and obtain transparent results even in the steady state ρ_s, which obeys the equation $\hat{L}\rho_s=0$. The incident classical electric field with frequency ω_0 and wave number κ propagating along z axis is given by

$$\boldsymbol{E}(z,t) = \mathcal{E}(z,t)e^{-i(\omega_0 t-\kappa z)} + c.c. \tag{4}$$

We split it into right (σ^+) and left (σ^-) circularly polarized components according to

$$\mathcal{E} = \mathcal{E}_+\boldsymbol{\epsilon}_+ + \mathcal{E}_-\boldsymbol{\epsilon}_-, \tag{5}$$

where $\boldsymbol{\epsilon}_\pm=(\hat{\boldsymbol{x}}+i\hat{\boldsymbol{y}})/\sqrt{2}$ are the unit circular polarization vectors. The minimal basis $\{e_i\}$ for the $j_1=1/2-j_2=1/2$ atom consists of eight following elements:

$$e_i = e_{ii}(00) = \frac{1}{\sqrt{2j_i+1}}\sum_{m_i}|j_im_i\rangle\langle j_im_i|, \quad i=1,2,$$

$$e_3 = \sum_m (-1)^m(\hat{z})_{-m}e_{11}(1m),$$

$$e_4 = \sum_m (-1)^m(\hat{z})_{-m}e_{22}(1m),$$

$$e_5 = e_6^\dagger = \sum_m (-1)^m(\boldsymbol{\epsilon}_+)_{-m}e_{12}(1m),$$

$$e_7 = e_8^\dagger = \sum_m (-1)^m(\boldsymbol{\epsilon}_-)_{-m}e_{12}(1m), \tag{6}$$

where

$$e_{ik}(jm) = \sum_{m_im_k}(-1)^{j_i-m_i}C(j_kj_ij;m_k,-m_i,m)|j_km_k\rangle\langle j_im_i|. \tag{7}$$

The details of the construction are given in [22]. The kets $|j_im_i\rangle$, $i=1,2$, denote the atomic states (1 refers to the ground state, 2 to the upper one). The symbol $C(j'j''j;m',m'',m)$ is a Clebsch-Gordan coefficient. The corresponding angular momenta and their projections are denoted by j_k and m_k.

The reduced density matrix of the atomic system is described by the components ρ_i, $i=1,\ldots,8$ [cf. Eq. (1)], which have well-defined physical meanings. The first two ones are related to the populations of the states labeled by 1 and 2 as follows: $p_1=\sqrt{2}\rho_1$, $p_2=\sqrt{2}\rho_2$. The orientation in the ground and excited states are equal to $\sqrt{2}\rho_3$ and $\sqrt{2}\rho_4$, respectively. Therefore the average value of the total angular-momentum operator is given by

$$\langle \boldsymbol{J} \rangle = \frac{1}{\sqrt{2}}(\rho_3+\rho_4)\hat{z}. \tag{8}$$

The atomic coherences between the states 1 and 2 are represented by the rest of the components.

If we write the atomic dipole operator as

$$\boldsymbol{\mu_D} = \boldsymbol{d} + \boldsymbol{d}^\dagger, \tag{9}$$

where $\boldsymbol{d}$ represents its rising part corresponding to the $1 \to 2$ transition, we obtain [22]

$$\boldsymbol{\epsilon}_\pm \cdot \boldsymbol{d} = \frac{1}{\sqrt{3}}\langle 2\|d\|1\rangle \sum_m (-1)^m (\boldsymbol{\epsilon}_\pm)_{-m} e_{12}(1m). \tag{10}$$

The reduced matrix element of the dipole moment operator is denoted by $\langle 2\|d\|1\rangle$.

We rewrite the interaction (3) using elements of the basis (6),

$$V = (v_+ e_5 + v_- e_7)e^{-i(\omega_0 t - \kappa z)} + h.c., \tag{11}$$

where v_+ and v_- denote the couplings between the atom and the respective circularly polarized field components (the Rabi frequencies are equal to $\sqrt{2}v_+$ and $\sqrt{2}v_-$). When $v_+ = v_-$ the light polarization is linear with the coupling $v_L = \sqrt{2}v_\pm$ (the Rabi frequency equals to $\sqrt{2}v_L$).

We calculate the matrix $A=-i(e_i,\hat{L}e_j)=-i\,\mathrm{Tr}(e_i^\dagger \hat{L} e_j)$, which governs the evolution of the density matrix [cf. Eq. (2)] in the framework of the RWA,

$$\frac{d\rho_i}{dt} = \sum_j A_{ij}\rho_j, \tag{12}$$

where

$$A = \begin{pmatrix} 0 & \gamma & 0 & 0 & \tilde{v}_+^* & \tilde{v}_+ & \tilde{v}_-^* & \tilde{v}_- \\ 0 & -\gamma & 0 & 0 & -\tilde{v}_+^* & -\tilde{v}_+ & -\tilde{v}_-^* & -\tilde{v}_- \\ 0 & 0 & 0 & -\gamma/3 & -\tilde{v}_+^* & -\tilde{v}_+ & \tilde{v}_-^* & \tilde{v}_- \\ 0 & 0 & 0 & -\Gamma_2^{(1)} & -\tilde{v}_+^* & -\tilde{v}_+ & \tilde{v}_-^* & \tilde{v}_- \\ -\tilde{v}_+ & \tilde{v}_+ & \tilde{v}_+ & \tilde{v}_+ & -\Gamma+i\Delta & 0 & 0 & 0 \\ -\tilde{v}_+^* & \tilde{v}_+^* & \tilde{v}_+^* & \tilde{v}_+^* & 0 & -\Gamma-i\Delta & 0 & 0 \\ -\tilde{v}_- & \tilde{v}_- & -\tilde{v}_- & -\tilde{v}_- & 0 & 0 & -\Gamma+i\Delta & 0 \\ -\tilde{v}_-^* & \tilde{v}_-^* & -\tilde{v}_-^* & -\tilde{v}_-^* & 0 & 0 & 0 & -\Gamma-i\Delta \end{pmatrix} \tag{13}$$

and $\tilde{v}_\pm = v_\pm/\sqrt{2}$, $\Delta=\omega_0-\omega_{21}$ (ω_{21} is the energy gap between the ground and excited level). We have assumed implicitly that both circular components have the same carrier frequency. In general, a carrier frequencies difference, frequency sweeping, or chirping can be described by phase factors of $v_\pm$. The spontaneous decay rate of the excited state is given by γ, the damping of the orientation in this state is described by the rate $\Gamma_2^{(1)}=\gamma+\gamma_{22coll}$, and the damping rate of the atomic coherences is given by $\Gamma=\gamma/2+\gamma_{12coll}$. The subscript *coll* labels the collisional damping rates. During evolution the normalization condition

$$\sqrt{2}\rho_1 + \sqrt{2}\rho_2 = 1 \tag{14}$$

is fulfilled.

In the model presented in [15,16] the propagation of the circularly polarized light components in the medium with N optically active atoms per unit volume is described by

$$\frac{\partial}{\partial z}v_+(z,\tau) = \alpha' \rho_5(z,\tau), \tag{15}$$

$$\frac{\partial}{\partial z}v_-(z,\tau) = \alpha' \rho_7(z,\tau), \tag{16}$$

where $\alpha'=2\pi N\omega_0\langle 2\|d\|1\rangle^2/(3c)$ and $\tau=t-z/c$ is retarded time. Since the Doppler effect is neglected we do not perform the average over the atomic velocity distribution on the right-hand side of Eqs. (15) and (16).

The system of Eqs. (15) and (16) separates, i.e., both circular components propagate independently, in two cases,

(i) when the relaxation rates can be omitted, which is possible for very short pulses,

(ii) when the light field is so weak that the population of the upper level is negligible ($\rho_2(z,\tau) \ll 1$).

In both cases analytical solutions can be obtained [1]. We want to study the pulse and the free-induction field together; therefore we analyzed analytically only the second case.

III. AREA OF THE RINGING FIELD

At first let us consider the propagation of the pulses in the medium in which each atom is identically excited (like in the model of Burnham and Chiao [13]). We denote $\rho_+=\rho_5$ and

$\rho_- = \rho_7$. The evolution equations for these two coherences when $\rho_2(z,\tau) \ll 1$, i.e., in the weak filed limit, can be written in the form

$$\frac{\partial}{\partial \tau}\rho_\pm(z,\tau) = (-\Gamma + i\Delta)\rho_\pm(z,\tau) - \frac{v_\pm(z,\tau)}{2}. \tag{17}$$

Since the upper-state population is negligible the orientations $\sqrt{2}\rho_3 = \sqrt{2}\rho_4 = 0$.

Let us assume that the pulses are switched on at $\tau=0$ and that exist small initial coherences $\rho_\pm(z,\tau=0)=\rho_{\pm 0}$. We solve Eq. (15)–(17) using the Laplace transform technique [11,28] and obtain

$$\begin{aligned} v_\pm(z,\tau) = v_\pm(0,\tau) - \frac{\sqrt{2\alpha' z}}{2}\int_0^\tau d\tau' v_\pm(0,\tau') e^{-(\Gamma+i\Delta)(\tau-\tau')} \\ \times J_1(\sqrt{2\alpha'(\tau-\tau')z})/\sqrt{\tau-\tau'} \\ + \sqrt{2\alpha' z}\rho_{\pm 0} e^{-[(\Gamma+i\Delta)\tau]} J_1(\sqrt{2\alpha' \tau z})/\sqrt{\tau'}, \end{aligned} \tag{18}$$

where J_1 denotes the Bessel function of first order.

In order to calculate the ringing which is produced when a resonant light pulse propagates through a medium, Burnham i Chiao [13] assumed that each atom of the medium is excited by a Dirac δ-function incident pulse. It means that an initial coherence (in our case $\rho_{\pm 0}$) and population difference in all medium atoms was prepared. Using method described in [13] we can evaluate a weak ringing field produced by a small area or area close to 2π input δ-function pulses. This field is given by the third term on the right-hand side of Eq. (18).

It is well known that the Bloch equations for the two-level atom without relaxation terms can be solved analytically for any resonant pulse envelope [9]. System (12) can be also solved analytically under such assumptions. If we assume that $\rho_2(z,0)=0$, the final upper-level population and atomic coherence after passage of the pulse is given by

$$\sqrt{2}\rho_2(z,\tau\to\infty) = \frac{1}{2}\left(\sin^2\frac{\theta_+}{2} + \sin^2\frac{\theta_-}{2}\right),$$

$$\rho_\pm(z,\tau\to\infty) = -\frac{1}{2\sqrt{2}}\sin\,\theta_\pm, \tag{19}$$

where $\theta_\pm = \sqrt{2}\int_0^\infty v_\pm(\tau)d\tau$ is the pulse area. Moreover if $\rho_3(z,0)=0$, the final orientations are

$$\sqrt{2}\rho_3(z,\tau\to\infty) = \sqrt{2}\rho_4(z,\tau\to\infty) = -\frac{1}{4}(\cos\,\theta_+ - \cos\,\theta_-). \tag{20}$$

For small area the coherence [Eq. (19)] is proportional to the pulse area $[\rho_\pm(z,\tau\to\infty) \approx -\frac{1}{2\sqrt{2}}\theta_\pm]$. Following Burnham i Chiao [13] we calculate an area $\theta_{\pm R}$ of the weak ringing field by integration of the third term on the right-hand side of Eq. (18) over time. When the δ pulse has a small area we obtain

$$\theta_{\pm R}(z) = -\theta_\pm(1 - e^{-\alpha'/(2\Gamma)z}). \tag{21}$$

When the δ-pulse area is close to 2π the coherence prepared in the medium is proportional to the difference between 2π and pulse area $[\rho_\pm(z,\tau\to\infty) \approx \frac{1}{2\sqrt{2}}(2\pi - \theta_\pm)]$ and the area of the ringing field is given by

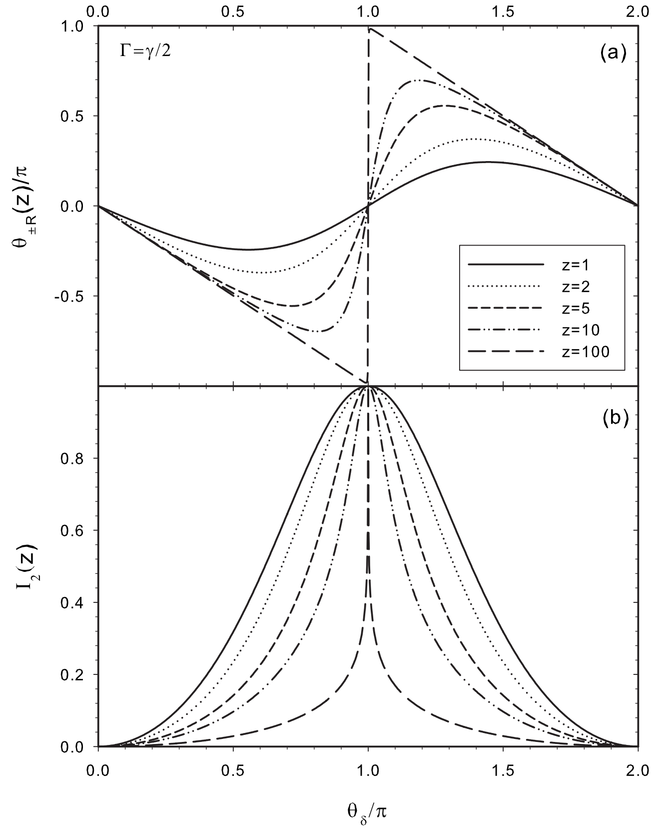

FIG. 1. The ringing field area and integral of the upper-level population as a function of the incident linearly polarized ($v_+ = v_-$) δ-function pulse area for several propagation distances.

$$\theta_{\pm R}(z) = (2\pi - \theta_\pm)(1 - e^{-\alpha'/(2\Gamma)z}). \tag{22}$$

The area $\theta_{\pm R}(z)$ can be also estimated when the medium is prepared by the linearly polarized ($v_+ = v_-$) δ pulse with the area close to π. In such a case the medium is inverted $[\sqrt{2}\rho_2(z,\tau) \approx 1]$. Repeating the procedure presented in [13] we get the formula for the ringing field area for very small propagation distances $[\alpha' z/(2\Gamma) \ll 1]$,

$$\theta_{\pm R}(z) = (\theta_\pm - \pi)\frac{\alpha'}{2\Gamma}z. \tag{23}$$

Analyzing Eqs. (21)–(23) and the results presented in [15,16] we expect that the ringing field area should add to the δ-function pulse area to give for large enough propagation distances total $2n\pi$ value and that in the vicinity of π the area $\theta_{\pm R}(z)$ abruptly changes sign. We have verified this hypothesis solving numerically Eqs. (12), (15), and (16) for the linearly polarized light ($v_+ = v_-$) described by $v_L = \sqrt{2}v_\pm$. We use the integration procedure proposed in [4]. We have chosen as a time unit $\tau_0 = 1/\gamma$ and as a unit of distance $z_0 = 2\Gamma/\alpha'$. The δ-function pulse produces initial state of the medium atoms according to Eq. (19). We have assumed that only spontaneous relaxation is present. The results supporting our hypothesis are showed in Fig. 1(a). The smaller is the

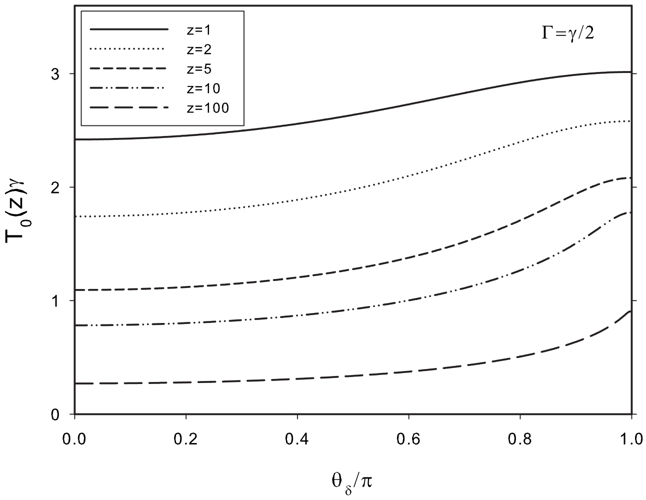

FIG. 2. The ringing field mean duration [Eq. (25)] as a function of the incident linearly polarized ($v_+=v_-$) δ-function pulse area for several propagation distances.

δ-function pulse area, the faster its correlation with the ringing field area is achieved. This correlation process is accompanied by the reduction in the losses due to spontaneous emission, which are proportional to the integral of the upper-level population,

$$I_2(z) = \gamma\sqrt{2}\int_0^\infty \rho_2(z,\tau)d\tau \tag{24}$$

[see Fig. 1(b)]. When the medium is prepared by the π pulse, the ringing is absent and the losses are highest. Whole energy transferred to the medium is spontaneously re-emitted [$I_2(z)=1$]. For other δ-function pulse areas the energy of the ringing increases during propagation.

It was observed that FID decays faster than $1/\Gamma$ and that its lifetime is sensitively dependent on the propagation distance [8]. Formula (18) is valid only for weak δ-function pulses. For stronger pulses the analytical dependence on time of the ringing is unknown. Since it is difficult to define its lifetime we adopt the concept of the equivalent pulse [16]. We are looking for a rectangular pulse having the same absolute area and energy as the ringing field. The duration of such pulse is given by

$$T_0 = \left[\int |v_\pm(\tau)|dt\right]^2 \Big/ \int |v_\pm(\tau)|^2 dt. \tag{25}$$

We have calculated the FID lifetime for the situation presented in Fig. 1. Since $\Gamma=\gamma/2$ we have expected that T_0 should be close to $2/\gamma$ at least for small area δ-function input pulses and small propagation distances. It was found that the ringing duration is nearly $2.5/\gamma$ for weak pulses and $z=z_0$ (Fig. 2). It grows monotonically and achieves value slightly larger then $3/\gamma$ for θ_δ tending to π. Obviously for $\theta_\delta=\pi$ the lifetime T_0 is undefined. The ringing duration decreases during propagation with the rate depending on the incident pulse area (see Fig. 2).

IV. PROPAGATION OF CIRCULARLY POLARIZED PULSES

When circularly polarized cw-laser field excites the $j_1=1/2-j_2=1/2$ atom, the orientation in the ground state ($O_g=\sqrt{2}\rho_3$) appears due to the optical pumping effect. Since the damping of this orientation is negligible the medium composed of such atoms becomes transparent. Obviously the orientation produced by a propagating pulse should depend on pulse parameters, properties of the medium, and propagation distance. Weak pulses or short pulses (compare to the lifetime) with area close to $2n\pi$ generate a negligible orientation. It is expected that the effect of optical pumping with long pulses or short pulses inverting the medium [$(2n+1)\pi$-pulse] should be significant. The orientation in the ground level depends on the integrated upper-level population. Therefore all processes which diminish the integral I_2 decrease the final orientation. The pulse plus ringing area stabilization is one of such processes. In general, the generation of the orientation diminishes the number of optically active atoms, which influences the propagation of the pulse and ringing.

We have solved numerically the propagation [Eqs. (15) and (16)] assuming that the input pulse envelope is given by the quadratically switched on Gaussian function (QG),

$$v_\pm(0,\tau) = \frac{64}{27}\sqrt{2}\pi v_{0\pm}\left(\frac{\tau}{T}\right)^2 \exp\left[-\frac{8}{9}\pi\left(\frac{\tau}{T}\right)^2\right], \tag{26}$$

where the parameters $v_{0\pm}$ and T can be understood as mean pulse coupling and duration

$$v_{0\pm} = \int_0^\infty v_\pm(0,\tau)^2 d\tau \Big/ \int_0^\infty v_\pm(0,\tau)d\tau, \tag{27}$$

$$T = \left[\int_0^\infty v_\pm(0,\tau)d\tau\right]^2 \Big/ \int_0^\infty v_\pm(0,\tau)^2 d\tau. \tag{28}$$

The obtained results [Fig. 3(a)] show that the optical pumping weakly influences the short pulse area stabilization effect. The circularly polarized pulse ($\theta_+\neq 0$ and $\theta_-=0$) area achieves 2π or 0π slightly earlier than linearly polarized one ($\theta_+=\theta_-$). For small distances one can treat the propagation of such a short pulse and the ringing field as nearly independent. The pulse propagates practically unchanged and the area of ringing increases or decreases forming together with the pulse the $2n\pi$ pulse [15]. Due to the optical pumping the density of atoms which can be excited decreases in time when they are driven by circularly polarized light. Therefore the leading edge of the pulse propagates in more dense optically active medium than the ringing which results in earlier stabilization of the circularly polarized field in comparison with the linearly polarized one.

It is apparent that there exists a relation between the pulse area and pulse energy. In our model the pulse energy is dissipated due to the spontaneous emission of medium atoms only. Therefore the nonzero pulse area cannot be constant during propagation. So it is not strange that the circularly or linearly polarized 2π pulse transforms into 0π pulse [Fig. 3(a)]. Since the optical pumping decreases the optically ac-

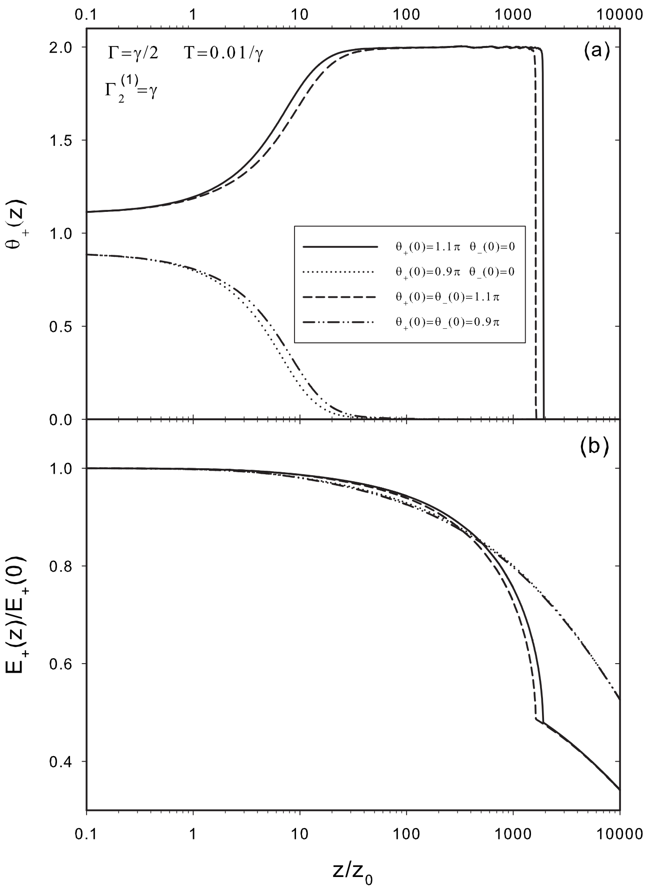

FIG. 3. (a) The pulse area θ_+ and (b) relative energy vs propagation distance for different input QG pulse area and polarization.

tive atoms density, the circularly polarized 2π pulse loses energy slower and is transformed later than the linearly polarized one. The behavior of the relative pulse energy [Fig. 3(b)] confirms this statement.

The energy of the pulses transforming themselves into the 0π pulses behaves smoothly and practically does not depend on pulse polarization. The behavior of the 2π pulses is more dramatic. The acceleration of the losses in the transformation region can be observed. However, generated 0π pulses lose their energy much slower [cf. Fig. 3(b)].

Since the ground-state final orientation is related to the pulse energy dissipation $[O_g(z,\infty)=\frac{2}{3}I_2(z)]$, the large increase in the losses in the transformation region should be accompanied by an increase in this orientation. In Fig. 4 we present the distribution of the orientation along the propagation distance of the circularly polarized pulses transforming into 2π and 0π pulses. As it is expected the orientation decreases with propagation distance but grows rapidly when the 2π pulse is destroyed. Its maximal value achieves nearly 0.4 which is larger than the value of the orientation produced by any pulse with the same duration and envelope for $z=0$ [compare Fig. 5(b)]. It is also more than the value 1/3 created by the circularly polarized δ-function pulse emptying one of the Zeeman sublevels of the ground state.

It seems that at least for short pulses (of the order of $0.01/\gamma$), the total pulse area stabilization process does not

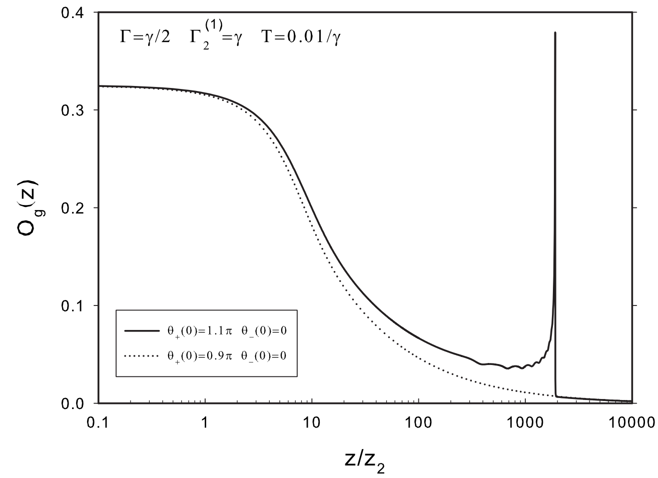

FIG. 4. The ground-state orientation vs propagation distance for two input circularly polarized QG pulse areas.

depend strongly on the light polarization. The decrease in the number of optically active atoms due to the optical pumping does not change qualitatively the relation between the input and output pulse areas [compare Fig. 5(a)]. The results are similar to obtained for linearly polarized light [15]. One can observe formation of the steps characteristic for the area theorem [2].

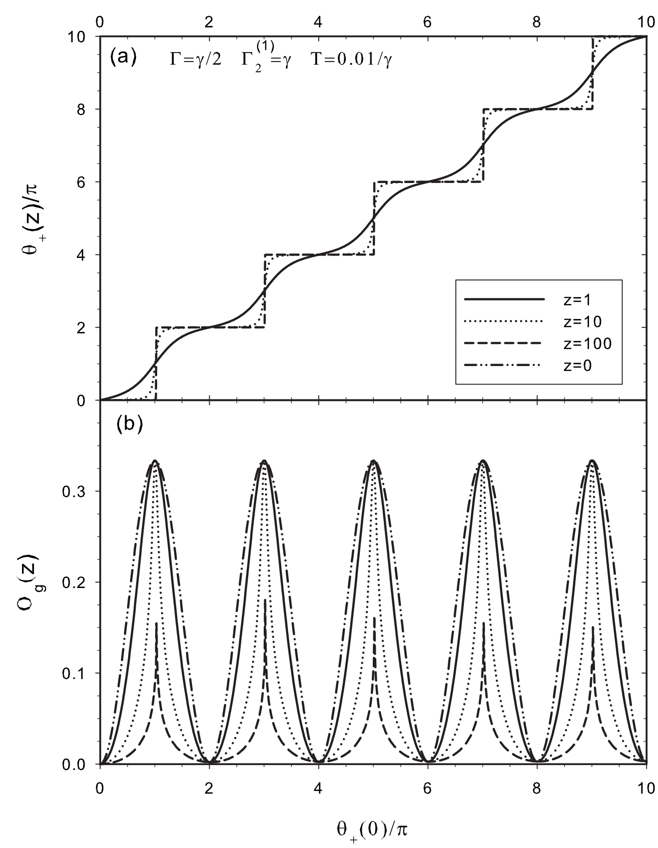

FIG. 5. (a) The output area of the circularly polarized light and (b) final ground-state orientation vs the input short QG pulse area for different values of the propagation distance.

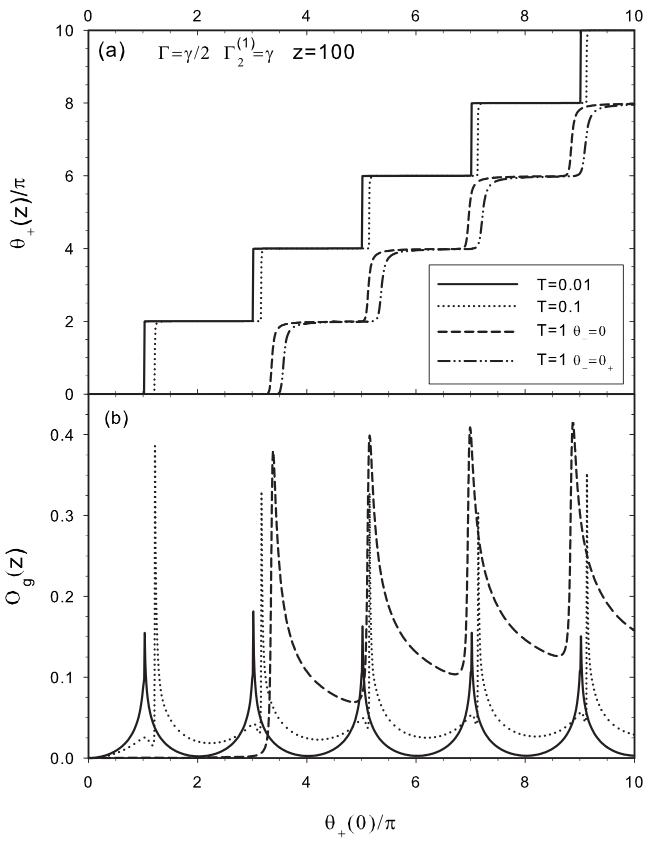

FIG. 6. (a) The output area of the circularly polarized light and (b) final ground-state orientation vs the input QG pulse area for different pulse durations and polarizations.

The final lower-state orientation changes periodically with incoming pulse area and decreases with propagation distance [Fig. 5(b)]. However one can expect large increase in the orientation in the transition region, where $2n\pi$ pulse becomes $2(n-1)\pi$.

Obviously, the ground-state orientation $O_g(z)$ equals 1 for the cw-laser field. Therefore the longer the pulse is, the larger orientation should be produced. A long linearly polarized pulse is strongly influenced by the propagation but still one can observe the pulse area stabilization [15]. Only the symmetry between input and output areas is removed. The similar asymmetry is observed for circularly polarized pulses [see Fig. 6(a)]. The long pulses need more input area than short ones to stabilize their areas on the $2n\pi$ level. A significant difference between the propagation of the linearly and circularly polarized pulse appears for pulses with duration in the order of $1/\gamma$. The stable circularly polarized 2π pulse is generated for the smaller input areas than for the linearly polarized one.

The relation between final ground-state orientation and input pulse area loses its symmetry when the pulse duration grows up. The peaks of the maximal orientation are not only shifted in direction of the large input areas but they become asymmetric. As it is expected, long pulses in general produce larger orientation.

V. REDISTRIBUTION OF ENERGY BETWEEN COMPONENTS OF ELLIPTICALLY POLARIZED LIGHT

A. Steady state propagation

Two circularly polarized pulses with orthogonal polarizations and with the same carrier frequency compose in general elliptically polarized one. During propagation in the $j_1=1/2-j_2=1/2$ medium, they are coupled only by the spontaneous decay process and there is no exchange of energy between them. Delagnes and Bouchene [17] presented different approach to this problem. They studied the propagation of two linearly polarized pulses with orthogonal polarizations (say along x and y axes, respectively). They assumed that there exists a relative phase $\phi(z=0)$ between the pulses at the entrance of the medium.

In order to describe their experimental setup in the framework of our formalism, we put $v_{x(y)}=|v_{x(y)}|e^{i\phi_{x(y)}}$ and $\phi=\phi_x-\phi_y$, then using Eqs. (15) and (16) and relations

$$v_+=\frac{1}{\sqrt{2}}(v_x-iv_y), \tag{29}$$

$$v_-=\frac{1}{\sqrt{2}}(v_x+iv_y), \tag{30}$$

we can derive equations describing the steady-state propagation of the components v_x and v_y,

$$\frac{d|v_x|^2}{dz}=\sqrt{2}\alpha'\ \mathrm{Re}[v_x^*(\rho_++\rho_-)], \tag{31}$$

$$\frac{d|v_y|^2}{dz}=-\sqrt{2}\alpha'\ \mathrm{Im}[v_y^*(\rho_+-\rho_-)], \tag{32}$$

$$\frac{d\phi}{dz}=\frac{\alpha'}{\sqrt{2}}\left\{\mathrm{Im}\left[\frac{1}{v_x}(\rho_++\rho_-)\right]-\mathrm{Re}\left[\frac{1}{v_y}(\rho_+-\rho_-)\right]\right\}. \tag{33}$$

Solving the set of Eq. (13) for the steady state we obtain from Eqs. (31)–(33),

$$\frac{d|v_x|^2}{dz}=\frac{\alpha'\gamma|v_x|^2}{D}[-\Gamma(|v_x|^2+|v_y|^2\cos 2\phi)-\Delta|v_y|^2\sin 2\phi], \tag{34}$$

$$\frac{d|v_y|^2}{dz}=\frac{\alpha'\gamma|v_y|^2}{D}[-\Gamma(|v_y|^2+|v_x|^2\cos 2\phi)+\Delta|v_x|^2\sin 2\phi], \tag{35}$$

$$\frac{d\phi}{dz}=\frac{\alpha'\gamma}{D}\left[\frac{\Gamma}{2}(|v_x|^2+|v_y|^2)\sin 2\phi-(|v_x|^2-|v_y|^2)\Delta\ \sin^2\phi\right], \tag{36}$$

where

$$D=2\Gamma(|v_x|^4+2|v_x|^2|v_y|^2\cos 2\phi+v_y^4)+\gamma(\Gamma^2+\Delta^2)(|v_x|^2+|v_y|^2)>0.$$

Treating the field described by v_x as a probe and v_y as a pump one, we can find the steady-state probe field

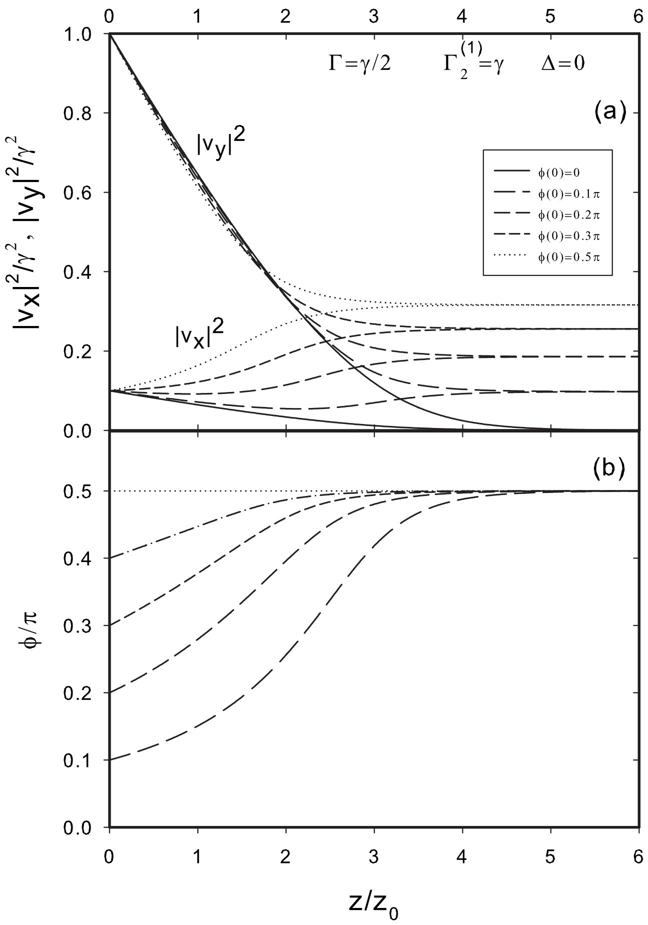

FIG. 7. (a) The equalization of the intensities of the resonant v_x and v_y components and (b) growth of the initial relative phase due to the stationary propagation. $|v_y(0)|^2=10|v_x(0)|^2=\gamma^2$.

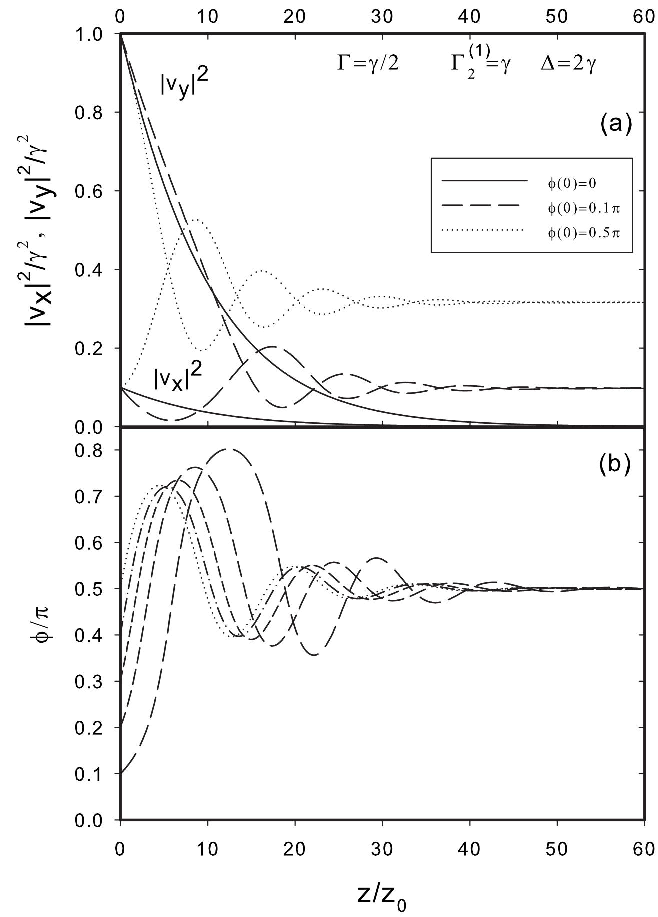

FIG. 8. (a) The equalization of the intensities of the detuned v_x and v_y components and (b) the change of the initial relative phase due to the stationary propagation. $|v_y(0)|^2=10|v_x(0)|^2=\gamma^2$.

amplification/absorption rate g_x defined by $d|v_x|^2/dz = g_x|v_x|^2+\ldots$,

$$g_x = -\frac{\alpha\gamma}{2\Gamma|v_y|^2+\gamma(\Gamma^2+\Delta^2)}(\Gamma\cos 2\phi+\Delta\sin 2\phi). \tag{37}$$

As it is expected this rate exhibits 2ϕ periodicity due to the interference effect described in [17] if only the phase change during propagation is negligible. In the resonance regime ($\Delta=0$) the probe field amplification is possible when $\cos 2\phi<0$ and is most efficient for $\phi=\pi/2$. Moreover if we assume that the pump field is relatively weak, i.e., $|v_y| \ll \sqrt{\gamma\Gamma}$, coherent control of the medium susceptibility is possible [29].

Obviously the increase in the v_x component intensity is due to the energy transfer from the v_y one. If we assume that $\Delta=0$ it is immediately seen from Eqs. (34)–(36) that during the steady-state propagation, the phase ϕ initially not equal to $k\pi/2$ tends monotonically to $k\pi/2$ and $|v_x|^2\to|v_y|^2$ (compare Fig. 7). The final value of $|v_x|^2$ and $|v_y|^2$ is given by the steady-state propagation constant,

$$|v_x(z)|^2|v_y(z)|^2\sin^2\phi(z) = |v_x(0)|^2|v_y(0)|^2\sin^2\phi(0), \tag{38}$$

obtained from Eqs. (34)–(36). In other words initially elliptically polarized light transforms into circularly polarized one propagating without losses. If $\phi(0)=k\pi/2$, i.e., when the light is polarized linearly, both components are absorbed [see Fig. 7(a)]. When the driving light is detuned from the resonance, $\Delta\neq 0$, the intensities of both components and the relative phase oscillate before stabilization if only $\phi(0)\neq k\pi/2$ (see Fig. 8).

If instead of the v_x and v_y components we consider the $v_+=|v_+|e^{i\phi_+}$ and $v_-=|v_-|e^{i\phi_-}$ ones, we obtain much simpler propagation equations

$$\frac{d|v_\pm|^2}{dz} = -\frac{2\alpha'\gamma}{d}\Gamma|v_+|^2|v_-|^2, \tag{39}$$

$$\frac{d\phi_\pm}{dz} = \frac{2\alpha'\gamma}{d}\Delta|v_\mp|^2, \tag{40}$$

where

$$d = 8\Gamma|v_+|^2|v_-|^2+\gamma(\Gamma^2+\Delta^2)(|v_+|^2+|v_-|^2)>0.$$

Now

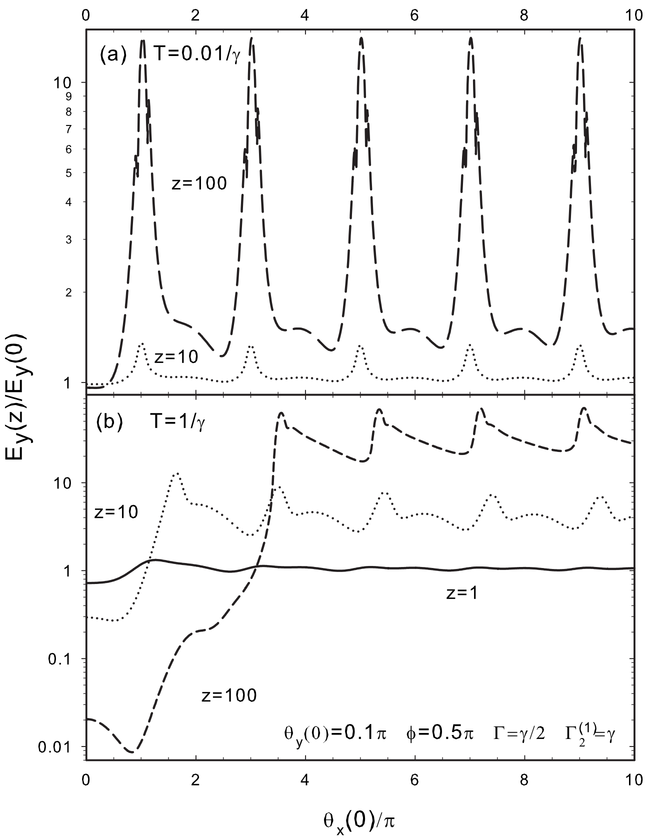

FIG. 9. The amplification of the resonant probe QG pulse polarized linearly along y axis as a function of the resonant QG pump pulse area. The pump pulse is polarized linearly in the x direction. (a) The short pulse and (b) long pulse amplification for several values of the propagation distance.

$$|v_+|^2 - |v_-|^2 = \text{const} \tag{41}$$

is conserved during propagation. Analysis of Eq. (39) shows that the intensities of circular components forming elliptically polarized light decrease monotonically. The intensity of the weaker one tends to zero and of the stronger one achieves the value given by Eq. (41). Using Eq. (40) one can calculate self-rotation angle $\phi_{SR}=(\phi_- - \phi+)/2$ of the detuned elliptically polarized light [30].

B. Resonant pulse propagation

Delagnes and Bouchene [17] investigated the propagation of femtosecond probe and pump pulses experimentally and numerically. They showed that the probe pulse amplification process depends essentially on the relative phase between linearly polarized pump and probe pulses but also periodically on the pump pulse area at the cell entrance. This periodicity was attributed to the Rabi oscillations.

Taking into account the results obtained for ultrashort pulses [17] and our steady-state results, one can expect that the amplification of the total pulse, i.e., the pulse plus the free-induction field, should exhibit features characteristic for short and long-time behavior. This supposition is, to some extent, justified by our numerical results which we present in Fig. 9. We have considered the most favorable relative phase between pulses entering the medium, i.e., $\phi(0,\tau)=\pi/2$ and we studied the resonant ($\Delta=0$) propagation of the QG probe pulse polarized along the y axis and having at $z=0$ area $\theta_y(0)=\sqrt{2}\int_0^\infty v_y(0,\tau)d\tau=0.1\pi$ (compare [17]). This pulse propagates in the presence of the resonant pump pulse with the same envelope, duration, and onset but polarized along x axes. We have studied how the relative probe pulse energy $E_y(z)/E_y(0)$ depends on the pump pulse input area $\theta_x(0)=\sqrt{2}\int_0^\infty v_x(0,\tau)d\tau$ (Fig. 9).

When both pulses are short with $T=0.01/\gamma$ [Fig. 9(a)] the probe pulse energy as a function of $\theta_x(0)$ exhibits periodicity. The amplification is maximal for the pump pulse input area in the vicinity of $n\pi$. Since we put $\phi(0)=\pi/2$ the relative phase is not changed during propagation, i.e., $\phi(z,\tau)=\pi/2$, and from Eqs. (29) and (30) we get

$$\theta_\pm(z) = \theta_x(z) \pm \theta_y(z). \tag{42}$$

Therefore we can treat the propagation of the linearly polarized probe and pump pulses as a propagation of two circularly polarized ones whose initial areas differ by $2\theta_y(0)$ and we can expect that their total areas will be stabilized and destabilized as described in Sec. IV. In the case presented in Fig. 9(a) $\theta_+(0)-\theta_-(0)=0.2\pi$ and in the vicinity of the maximums $\theta_+(0)>(2n+1)\pi$ whereas $\theta_-(0)<(2n+1)\pi$. It means that $\theta_+(0)\to 2n\pi$ and $\theta_-(0)\to 2(n-1)\pi$ in the course of the propagation and for a sufficiently large z the area difference $\theta_+-\theta_-\approx 2\pi$. Since relation (42) has to be fulfilled the area θ_y increases to π and θ_x decreases to $(2n-1)\pi$ in the transition region. In this way the amplification maximums showed in Fig. 9(a) appear. The subtle structures seen in Fig. 9(a) are due to the complex overlapping of the entering pulse and the ringing, and are not present when one studies the amplification of the pulse only, i.e., without ringing [17].

The amplification periodicity observed for the short pulses also exists when propagation of long pulses with $T=1/\gamma$ is investigated [Fig. 9(b)]. Since the stabilization of the long circularly polarized pulse area on $2n\pi$ level appears for relatively large input pulse areas (see Fig. 6), the onset of periodic pattern shifts to larger values of $\theta_x(0)$ when propagation distance increases. For the pulses with the input areas in the vicinity of the amplification maximums, there exist propagation distances at which these pulses have the same stabilized $\theta_\pm$ and a little further one of them transforms into a pulse with a lower stabilized area, i.e., $\theta_+-\theta_-\approx 2\pi$. According to Eq. (42) this change in the areas is accompanied by the increase in θ_y to π, and therefore the energy of the probe pulse grows up.

We have showed in previous subsection that the steady-state amplification of the probe field is very efficient. When $\phi=\pi/2$ the intensities of the probe and pump fields equalize quite quickly [see Eq. (35) and Fig. 7(a)]. Also the amplification of the long probe pulse with $T=1/\gamma$, which propagates in close to steady-state conditions, is more efficient than of the short one with $T=0.01/\gamma$ [compare Figs. 9(a) and 9(b)].

The probe pulse amplification mechanism related to the stabilization and destabilization of pulse area limits the energy which can be transferred from the pump pulse to the probe one (θ_y should be smaller than π). One can expect

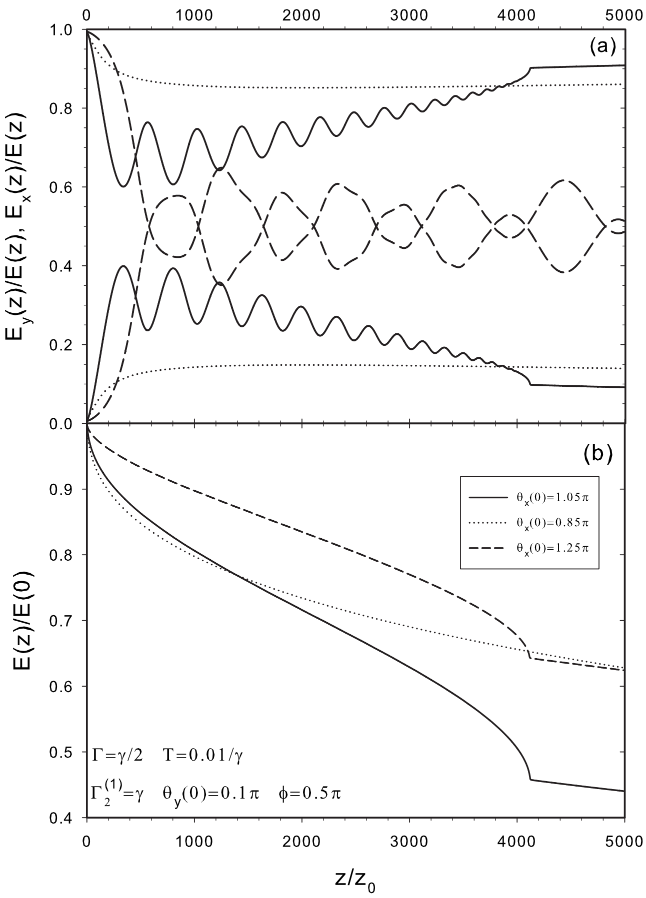

FIG. 10. The redistribution of the energy of the short elliptically polarized QG pulse between x and y components during propagation. (a) The relative energy of the components and (b) relative total energy vs propagation distance for different areas $\theta_x(0)$ of the input linearly polarized pump pulse.

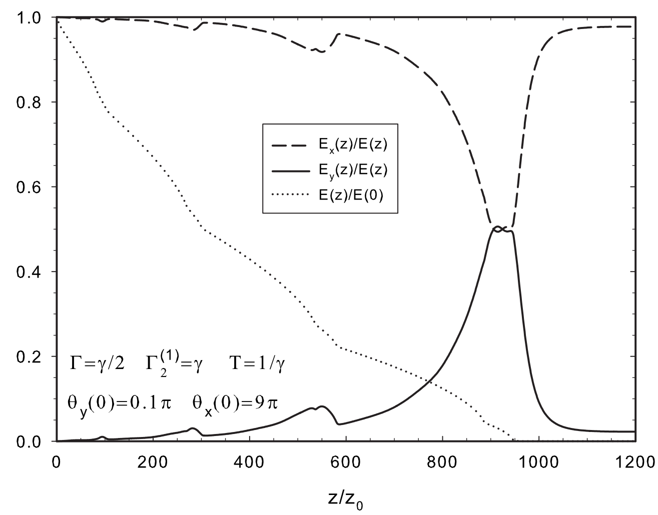

FIG. 11. The redistribution of the energy of the long elliptically polarized QG pulse between x and y components during propagation—the relative energy of the components and relative total energy vs propagation distance.

equalization of the energy of pulses only when the pump pulse is weak enough. In order to demonstrate this effect we have studied numerically the propagation of the pump pulses with $\theta_x(0)=0.85\pi$, 1.05π, and 1.25π (Fig. 10). We put $\theta_y(0)=0.1\pi$ and $\phi(0)=\pi/2$. These three cases illustrate three simplest situations: in the first one, both circularly polarized pulses are stabilized as 0π pulses, in the second one becomes the 2π and the other 0π pulse and in the third case we get two 2π pulses.

In all three cases the probe pulse contribution $E_y(z)/E(z)$ to the total energy $E(z)=E_x(z)+E_y(z)$ increases monotonically and pump pulse contribution $E_x(z)/E(z)$ decreases monotonically for small propagation distances ($z\leq 500z_0$) [see Fig. 10(a)]. Further their behavior is qualitatively correlated with the input circular pulses areas. When these pulses are stabilized as 0π pulses ($\theta_x(0)=0.85\pi$), the probe pulse energy contribution achieves the level close to $0.13E(z)$ and then decreases very slowly. Obviously the total relative energy of these pulses decays monotonically [compare Fig. 10(b)].

When one of the pulses becomes a 0π pulse and the second 2π pulse [$\theta_x(0)=1.05\pi$, Fig. 10(a)], one can observe damped oscillations of the contributions of pump and probe pulses to the total energy until the 2π pulse transforms into 0π one. The oscillations frequency and amplitude depends, in general, on the probe pulse area $\theta_y(0)$. The periodic exchange of the roles between pump and probe fields occurs when both pulses are stabilized as 2π pulse, where [$\theta_x(0)=1.25\pi$, Fig. 10(a)]. The acceleration of the total-energy dissipation when circularly polarized $2n\pi$ pulses are destabilized is clearly seen [Fig. 10(b)]. It should be noted that the oscillations of the pulse energies are due to the ringing and are not present when one collects light for times of the order of several T.

This nice picture changes when we consider the propagation of long pulses with $T=1/\gamma$. We have chosen a relatively large pump pulse area $\theta_x(0)=9\pi$ and the same as before probe pulse one $\theta_y(0)=0.1\pi$ (Fig. 11). In such a case the circularly polarized pulses contributing to elliptically polarized field pass several levels of the stabilization: 8π, 6π, 4π, and 2π to finish as weak 0π pulses. This process can be observed in the behavior of the probe and pump pulses contributions to the total energy (see Fig. 11). The probe pulse contribution slowly increases when its area is stabilized and quickly decreases in the transition region. It equalizes with the pump pulse contribution when one of the circularly polarized pulses transforms from 2π pulse into 0π pulse, whereas the other is still 2π one. Obviously the relative total energy decreases monotonically but the influence of the area stabilization is apparent.

Finally we have calculated how the pump pulse relative energy depends on the relative phase $\phi(0)$ at the entrance to the cell (Fig. 12). As it is expected (see [17] and (35)) the $2\phi(0)$ periodicity is clearly seen. The probe field is practically always amplified except a small region around $\phi(0)=0$ and π.

The results presented in [Fig. 12(a)] show once more that the amplification of short pulses with $T=0.01/\gamma$ strongly depends on the input pump pulse area. The local maximums noticeable for $z=100z_0$ are due to the free-induction field. In

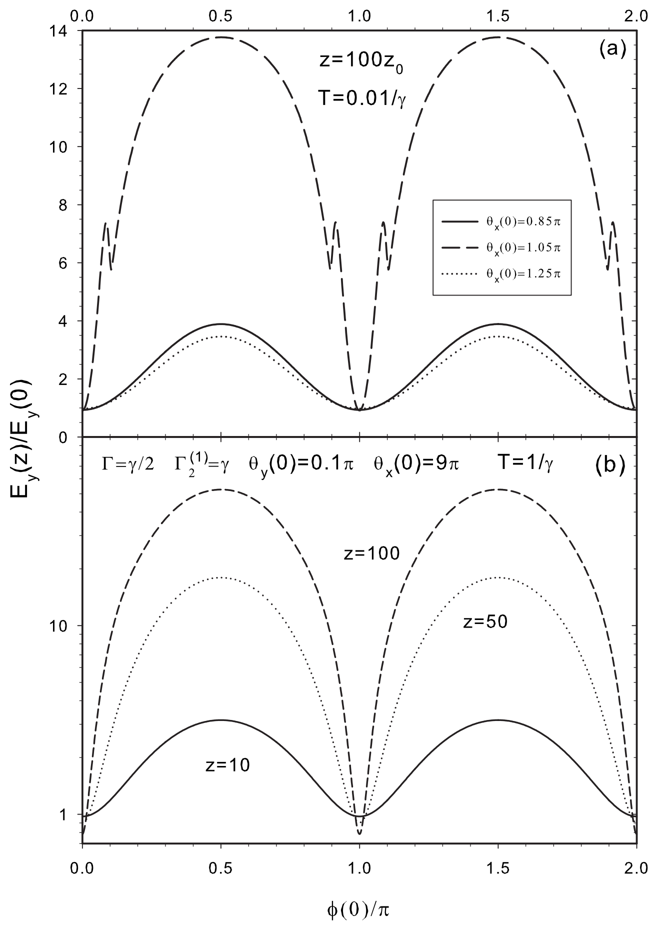

FIG. 12. The amplification of the probe QG pulse polarized linearly along y axis as a function of the relative phase $\phi(0)$. The pump QG pulse is polarized linearly in the x direction. (a) The short pulse amplification for three values of the pulse pump area and (b) the long pulse amplification for three values of the propagation distance.

general, the long pulse amplification is more efficient than short ones [compare Fig. 12(b) for $z=100z_0$ and Fig. 12(a)].

VI. SUMMARY

The propagation of short, in comparison with the atomic lifetime, light pulses is always accompanied by the free-induction field. The sharp-line model is most suitable for the study of the ringing properties. Due to the progress of the experimental techniques [7,8], the theoretical results obtained in the framework of this model can be now verified experimentally.

We have analyzed mainly numerically the propagation of two resonant light pulses with orthogonal circular polarizations in the medium composed of $j_1=1/2-j_2=1/2$ atoms. In general the superposition of these pulses gives elliptically polarized light. Since they couple two different pairs of Zeeman sublevels of the ground and excited states, this approach seems to be the most suitable for the description of the propagation of elliptically polarized light in such a medium. Obviously one can register different components of the propagating light, e.g., polarized linearly as in [17], but their properties are determined by their relation to the circularly polarized components.

Since the ringing decays in the time scale determined by the perpendicular relaxation the equations describing the atomic evolution should include relaxation rates and even in the case of very short pulses entering the medium the description unifying the pulse and free-induction field is necessary. Using such an approach in the framework of the fixed atoms approximation we have demonstrated the stabilization of the areas of circularly polarized components of the propagating pulse on the level $2n\pi$. Due to the spontaneous radiation losses this stabilization is not permanent. The area jumps down on the level $2(n-1)1\pi$ and finally achieves the value 0π. When the area is destabilized the radiation losses increases and the efficiency of the optical pumping by the propagating field increases.

When the pulse is very short and strong and the propagation distances small, the pulse and the ringing can be treated independently. In such a case the envelope of the pulse changes slightly during propagation but the ringing with the area adjusting total field area to the value $2n\pi$ arises. For long pulses and/or large propagation distances the pulse and the ringing cannot be distinguished but still the area stabilization occurs.

The elliptically polarized light was treated in [17] as a superposition of two linearly polarized fields with different phases. In this context the amplification of probe pulse in the presence of the pump one in the $j_1=1/2-j_2=1/2$ medium was considered. We have regarded this problem in more general manner studying redistribution of the energy between these components. We have derived the steady-state propagation equations for both field intensities and the relative phase. We have shown that the resonant elliptically polarized cw field transforms into circularly polarized one for which the medium is transparent.

Finally we have analyzed how the energy transfer between the pump and probe pulses. For the small propagation distances the simple probe pulse amplification occurs. When the energy of the probe pulse becomes comparable with the energy of the pump one complex process of energy exchange has been observed. The probe pulse amplification and energy transfer between pulses is strongly influenced by the area stabilization effect.

ACKNOWLEDGMENTS

Support by the Polish research network LFPPI is acknowledged.

[1] G. L. Lamb, Rev. Mod. Phys. **43**, 99 (1971).
[2] S. L. McCall and E. L. Hahn, Phys. Rev. Lett. **18**, 908 (1967).
[3] S. L. McCall and E. L. Hahn, Phys. Rev. **183**, 457 (1969).
[4] A. Icsevgi and W. E. Lamb, Phys. Rev. **185**, 517 (1969).
[5] H. M. Gibbs and R. E. Slusher, Phys. Rev. A **6**, 2326 (1972).
[6] M. Matusovsky, B. Vaynberg, and M. Rosenbluh, Phys. Rev. Lett. **77**, 5198 (1996).
[7] K. Toyoda, Y. Takahashi, K. Ishikawa, and T. Yabuzaki, Phys. Rev. A **56**, 1564 (1997).
[8] U. Shim, S. Cahn, A. Kumarakrishnan, T. Sleator, and J.-T. Kim, Jpn. J. Appl. Phys., Part 1 **41**, 3688 (2002).
[9] L. Allen and J. H. Eberly, *Optical Resonance and Two Level Atoms* (Wiley, New York, 1975).
[10] M. D. Crisp, Phys. Rev. A **1**, 1604 (1970).
[11] H.-J. Hartmann and A. Laubereau, J. Chem. Phys. **80**, 4663 (1984).
[12] R. G. Brewer and R. L. Shoemaker, Phys. Rev. A **6**, 2001 (1972).
[13] D. C. Burnham and R. Y. Chiao, Phys. Rev. **188**, 667 (1969).
[14] V. S. Egorov, V. N. Lebedev, I. B. Mekhov, P. V. Moroshkin, I. A. Chekhonin, and S. N. Bagayev, Phys. Rev. A **69**, 033804 (2004).
[15] A. Alhasan, J. Fiutak, and W. Miklaszewski, Z. Phys. B: Condens. Matter **88**, 349 (1992).
[16] W. Miklaszewski and J. Fiutak, Z. Phys. B: Condens. Matter **93**, 491 (1994).
[17] J. C. Delagnes and M. A. Bouchene, Phys. Rev. Lett. **98**, 053602 (2007).
[18] J. C. Delagnes and M. A. Bouchene, Phys. Rev. A **76**, 023422 (2007).
[19] J. C. Delagnes and M. A. Bouchene, Phys. Rev. A **76**, 045805 (2007).
[20] J. C. Delagnes and M. A. Bouchene, Phys. Rev. A **76**, 053809 (2007).
[21] C. Martin and L. W. Anderson, Phys. Rev. A **53**, 921 (1996).
[22] J. Fiutak and J. V. Kranendonk, J. Phys. B **13**, 2869 (1980).
[23] G. Hetet, A. Peng, M. T. Johnsson, J. J. Hope, and P. K. Lam, Phys. Rev. A **77**, 012323 (2008).
[24] Z. Kurucz and M. Fleischhauer, Phys. Rev. A **78**, 023805 (2008).
[25] K. Blum, *Density Matrix Theory and Application* (Plenum Press, New York, 1981).
[26] G. S. Agarwal, P. A. L. J.-P. Connerade, and S. West, J. Phys. B **30**, 5971 (1997).
[27] F. Schuller and D. N. Stacey, Phys. Rev. A **60**, 973 (1999).
[28] B. Macke, J. L. Queva, F. Rohart, and B. Segard, J. Phys. **48**, 797 (1987).
[29] F. A. Hashmi and M. A. Bouchene, Phys. Rev. Lett. **101**, 213601 (2008).
[30] S. M. Rochester, D. S. Hsiung, D. Budker, R. Y. Chiao, D. F. Kimball, and V. V. Yashchuk, Phys. Rev. A **63**, 043814 (2001).